

Fractal space-time: a geometric analogue of relativistic quantum mechanics

This article has been downloaded from IOPscience. Please scroll down to see the full text article.

1983 J. Phys. A: Math. Gen. 16 1869

(<http://iopscience.iop.org/0305-4470/16/9/012>)

View [the table of contents for this issue](#), or go to the [journal homepage](#) for more

Download details:

IP Address: 129.252.86.83

The article was downloaded on 30/05/2010 at 17:15

Please note that [terms and conditions apply](#).

Fractal space–time: a geometric analogue of relativistic quantum mechanics

G N Ord†

Department of Chemistry, University of Toronto, Toronto, Canada M5S 1A1

Received 13 September 1982, in final form 14 December 1982

Abstract. We consider a ‘thought experiment’ in which particles are confined to move on fractal trajectories in both space and time, treating the case of a Peano–Moore trajectory in detail. Generalising these results, we use the classical principle of relativity and a correspondence principle to show that fractal trajectories in space with Hausdorff dimension $D = 2$ exhibit both an uncertainty principle and a de Broglie relation. The incorporation of fractal time with $D = 2$ places an upper bound on the macroscopic velocities of ‘fractalons’, which in turn requires that the macroscopic physics be Lorentz covariant. On a microscopic scale, the presence of fractal time is interpreted in terms of the appearance of particle–antiparticle pairs when observation energies become of the order of mc^2 .

We propose two field equation descriptions of fractalons based on random walk space–time trajectories and subsequently relate these equations to the free particle Klein–Gordon and Dirac equations respectively.

1. Introduction

Newton’s first law states that every particle persists in a state of rest or uniform motion in a straight line, unless acted upon by an external force. However, as pointed out by Feynman (Feynman and Hibbs 1965), the paths of quantum mechanical particles look more like non-differentiable curves than straight lines when examined on a fine scale. Furthermore, relativistic interaction with particles at sufficiently high energies produces particle number non-conservation. As a result of these and other difficulties, quantum mechanics has traditionally abandoned the concept of a point particle and its attendant trajectory in favour of wavepackets or field excitations. An exception to this is provided by the path integral formulation of quantum mechanics (Feynman 1948) in which the particle trajectory plays an important role. One of the main advantages of this formulation is that it has strong intuitive appeal in its reference to a sum over continuous trajectories in space.

In light of this, a general question that one might ask is: to what extent may we construct continuous trajectories in space–time that exhibit features analogous to those found in relativistic quantum mechanics? In this paper we address this question by considering the physics of particles which are confined to move on fractal trajectories in space and time. Our motivation for doing this is to determine whether such a change in microscopic geometry yields any phenomena resembling quantum physics.

† Present address: Cornell University, Baker Laboratory, Ithaca, New York 14853, USA

The answer we obtain, while far from complete, is suggestive that such microscopic geometry may provide several features generally associated with relativistic quantum mechanics. We stress however that the article is not intended as a derivation of quantum mechanics. Rather it is intended to draw an identification between concepts arising from fractal space-time, and those existing in quantum mechanics.

The paper is organised as follows.

In § 2 we motivate the study of fractal space-time by investigating the motion of a particle confined to move on a particular fractal trajectory in space. We find that such a particle exhibits an uncertainty principle, but has an infinite instantaneous velocity, as in the case of a Brownian particle.

In § 3 we introduce fractal time. This places an upper bound on instantaneous velocities, at the expense of maintaining a single-particle interpretation in topologically one-dimensional time. We then propose 'idealised fractal space-time' and examine the phase diagram for free 'fractalons' in terms of scale. We notice that there are three phases corresponding to classical, quantum and field-like behaviour, depending on the scale of observation.

In § 4 we invoke a correspondence principle between the macroscopic and microscopic regime of fractalons. This, along with the classical relativity principle, yields a de Broglie relation between macroscopic momentum and 'fractal wavelength'. Furthermore, we see that the macroscopic physics must be Lorentz covariant.

In § 5 we discuss the space-time synchronisation implicit in previous sections and propose the use of a topologically six-dimensional space-time in which to embed fractal trajectories.

Finally, in § 6 we propose a simple random walk model of fractal space-time, and show that the resulting field equation may be related to the free-particle Klein-Gordon equation by a simple ansatz. We then show that a more detailed description of this model in one dimension yields the free-particle Dirac equation.

2. Fractal space

The term 'fractal' has been recently coined by Mandelbrot (1977) for objects whose topological and Hausdorff dimensions do not coincide. For an excellent exposition of the properties and uses of fractals we refer the reader to the above text.

In the following we shall use the Peano-Moore curve of figure 1 as a model of a fractal trajectory. We choose this curve because it is a simple example of a fractal with a Hausdorff dimension of 2, although any continuous fractal with $D = 2$ would lead to the same qualitative results.

Figures 1(a)-(c) show the trajectory of a hypothetical particle as finer detail is revealed through measurement with increasing precision. We shall assume that the particle traverses the distance AB in a time t_0 regardless of the scale on which the trajectory is examined. If we let

$$\eta_n = \lambda \left(\frac{1}{3}\right)^n \quad n = 0, 1, \dots$$

be the unit of measurement we find that (figure 1)

$$L_n = \lambda (\lambda / \eta_n) \quad \text{and} \quad v_n = v_0 (\lambda / \eta_n)$$

where L_n is the apparent length of the trajectory at a resolution η_n and v_n is the apparent speed of the particle.

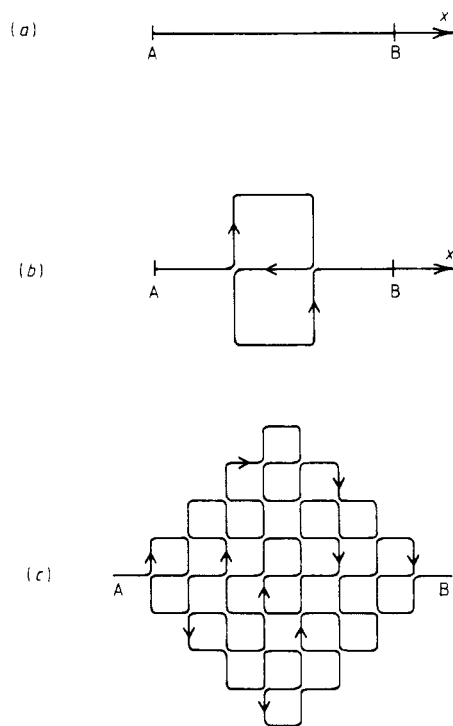


Figure 1. A particle's trajectory in space as observed with increasing resolution. Curves (a), (b) and (c) correspond to scales $\eta = \lambda$, $\eta = \lambda/3$ and $\eta = \lambda/9$ respectively.

Suppressing the n dependence of L and v , we may write

$$L(\eta) = \lambda (\eta/\lambda)^{1-D} \quad \eta \leq \lambda \tag{2.1}$$

$$v(\eta) = v_0 (\eta/\lambda)^{1-D} \quad \eta \leq \lambda. \tag{2.2}$$

Here, equation (2.1) serves to define the similarity dimension D which in this case is 2. (The relationship between similarity, fractal and Hausdorff dimension is discussed in Mandelbrot (1977). We shall use the terms interchangeably.)

We note that in general trajectories with different geometries will have different Hausdorff dimensions. The significance of the exponent $D = 2$ in (2.1) and (2.2) is that the Peano-Moore curve is essentially 'plane filling'. The usual rectifiable trajectories of classical physics would have $D = 1$.

We now consider the expected value of the x component of the velocity as a function of η . We do this by weighting each possible value of v_x according to the time spent with that particular velocity. For example, from figure (1b) we have

$$\langle v_x(\lambda/3) \rangle = \frac{4}{9}v(\lambda/3) + \frac{1}{9}[-v(\lambda/3)] + \frac{4}{9} \times 0 = v_0. \tag{2.3}$$

Similarly we expect in general

$$\langle v_x(\eta) \rangle = v_0 \quad \eta < \lambda.$$

However, if we now calculate $\langle v_x^2(\eta) \rangle$ we have for example

$$\langle v_x^2(\lambda/3) \rangle = \frac{4}{9}[v(\lambda/3)]^2 + \frac{1}{9}[-v(\lambda/3)]^2 + \frac{4}{9} \times 0^2 = \frac{5}{9}(3v_0)^2.$$

For $\eta < \lambda$ we thus expect

$$\langle v_x^2(\eta) \rangle \geq \frac{5}{9} v_0^2 (\eta/\lambda)^{2(1-D)}$$

so that

$$\Delta v_x(\eta) \equiv (\langle v_x(\eta) \rangle - \langle v_x'(\eta) \rangle)^2)^{1/2} \geq \frac{1}{3} \sqrt{5} v_0 [(\eta/\lambda)^{2(1-D)} - 1]^{1/2} \geq \frac{1}{3} \sqrt{5} v_0 (\eta/\lambda)^{1-D}.$$

Taking the uncertainty in x as η we have

$$\Delta x \Delta v_x \geq \frac{1}{3} \sqrt{5} v_0 (\eta/\lambda)^{1-D} \eta$$

so that for $D = 2$

$$\Delta x \Delta v_x \geq \frac{1}{3} \sqrt{5} v_0 \lambda. \tag{2.4}$$

Thus within the framework of our rather specialised measurement procedure, the product of the uncertainties in the x component of the velocity and the position of our hypothetical particle becomes independent of scale for $\eta < \lambda$, provided that the Hausdorff dimension of the trajectory is 2. By comparison, the fact that quantum mechanical particles move statistically on fractal paths with Hausdorff dimension 2 has been shown by Abbot and Wise (1980) and Campesino-Romeo *et al* (1982).

Apart from the rather implausible regularity of the above trajectory, our hypothetical particle has the unphysical attribute of an infinite instantaneous velocity (2.2). We shall remedy this situation in the next section.

3. Fractal time

Thus far we have assumed that time has both a topological and Hausdorff dimension of 1. Let us now suppose, by analogy with space, that temporal trajectories also have Hausdorff dimensions of 2, with fractal wavelengths τ , say, depending on the trajectory in question. Whereas a continuous fractal trajectory in space is easily pictured (figure 1), a continuous fractal trajectory in time requires an extra topological dimension in time for visualisation (figure 2). We shall consider this extra dimension to be unobservable directly. That is, we shall assume that an observer's clock has $\tau = 0$ and that a fractal trajectory in time appears as a projection onto one time axis.

Figure 2 shows a 'fractalon' on a time scale of $\tau/3$ with spatial and temporal fractal behaviour synchronised. On this scale the particle 'sees' a continuous trajectory in time of length $3\tau_1$ between a and d , as well as a spatial distance of $3\lambda^*$. However, an observer will see the projected time between a and d to be τ_1 . The fractal nature of time would seem to be manifest at point b by the 'destruction' of the original particle along with the 'creation' of three new particles. Two of these new particles appear exactly like the old particle except that they are displaced from the x axis. The third particle has the appearance of an 'antiparticle' moving along the x axis (its trajectory moves backwards in time from $t_1 = \frac{2}{3}\tau$ to $t_1 = \frac{1}{3}\tau$).

Thus on time scales below τ a single-particle description of fractalons breaks down if we restrict ourselves to a topologically one-dimensional time. We note, however, that if λ^* is the spatial scale at which fractal time is incipient, i.e. if

$$\lambda^*/v(\lambda^*) = \tau \tag{3.1}$$

and if $v_0 < w \equiv \lambda/\tau$ then $v(\lambda^*)$ is the maximum observable velocity of the fractalon

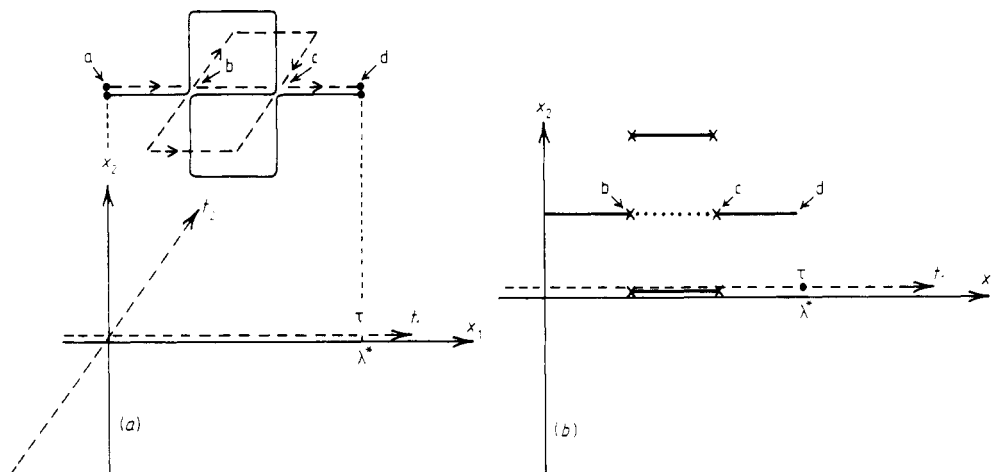


Figure 2. A fractal trajectory synchronised in space and time. (b) The trajectory with time projected onto the t_1 axis. Since the trajectory from c to b is traversed in the negative t_1 direction, we interpret this as an antiparticle traversing bc in the positive t_1 direction.

(e.g. in figure 2, $v(\lambda^*/3) = L(\lambda^*/3)/\tau_{ad}(\lambda^*/3) = 3L(\lambda^*)/3\tau_{ad}(\lambda^*) = v(\lambda^*)$ etc). Indeed, we may say that the fractalon (λ, v, w) corresponds to a particle that moves on a continuous fractal trajectory in space and time, with the constant velocity

$$c = \sqrt{vw} \tag{3.2}$$

on time scales below $\tau = \lambda/w$ where the time is measured on a ‘fractal clock’ with Hausdorff dimension 2 and wavelength τ . The maximum velocity $c = \sqrt{vw}$ is obtained by solving (3.1) for $v(\lambda^*)$. We note that this relation is the analogue of the equation relating the group and phase velocities of a wavepacket.

With the above particle–antiparticle interpretation we note that for our particular fractal trajectory the particle number is not conserved, although the number of particles minus the number of antiparticles, or the particle excess, is conserved and is always 1. Furthermore, for $v < w$ the process is continuous in the x direction in the sense that a particle excess of 1 has to ‘pass’ any given point on the x axis between a and d with finite velocity in observer time regardless of scale. If $v > w$ the situation is quite different (figure 3). Here the trajectory has gaps in it which are traversed by the fractalon in fractal time which is ‘lost’ through projection onto one dimension. Thus the particle excess which passes any given point on the x axis between a and d varies from point to point and is dependent on scale. We shall assume that such scale dependence fundamentally distinguishes fractalons with $v > w$ from fractalons with $v \leq w$ and shall consider only the latter type here.

In the following we set aside questions on the specific geometry of fractal trajectories and assume that fractalons possess an intrinsically synchronised space-time. We further assume the idealised behaviour of figure 5 so that free fractalons may be completely characterised by the ordered triple (λ, v, w) , specifying their wavelength, macroscopic velocity and phase velocity respectively. We shall discuss these assumptions in § 5.

Let us consider the set of fractalons

$$O_c = \{(\lambda, v, w) | \lambda, |v|, w > 0, v \leq w \text{ and } |v|w = c^2\} \tag{3.3}$$

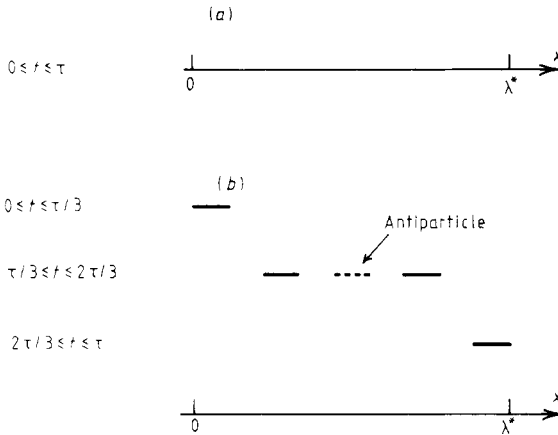


Figure 3. A fractal trajectory with $v > w$. (a) $\eta = \lambda^*$, the trajectory is continuous. (b) $\eta = \lambda^*/3 > \lambda$; here the length of the spatial trajectory has not changed from (a) although the velocity has dropped to $V(\lambda^*)/3$ leaving gaps in the particle trajectory.

where c is some positive number. We note that O_c is the set of all fractalons with maximum expected velocity c such that $v \leq c$.

Let T_u be a transformation to an inertial frame moving with constant speed $u < c$ in the x direction (figure 4). We wish to observe the effect of T_u on an arbitrary member of O_c , which we shall denote by $(\lambda, v)_c$. Since T_u is a kinematic transformation, it cannot change the fundamental character of a fractalon so that if

$$T_u(\lambda, v)_c = (\lambda', v')_{c'} \tag{3.4}$$

we must have $v' < c'$.

In order that $(\lambda, v)_c$ serve as a model of a free particle, we require that it have some representation (m_0, v) with m_0 an inertial mass and v a macroscopic velocity. The inertial mass will serve to identify the particle through changes in inertial frames, i.e.

$$T_u(m_0, v) = (m_0 v'). \tag{3.5}$$

Let us now propose the identification

$$(m_0, v) \leftrightarrow (\lambda, v)_c. \tag{3.6}$$

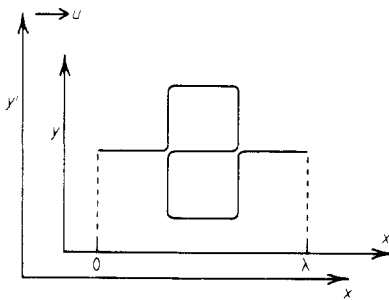


Figure 4.

This identification would imply that the particle (m_0, v) has a maximum expected velocity of c in the inertial frame in which its macroscopic velocity is v . If, however, the particle's maximum speed depends on its macroscopic velocity in an inertial frame, it may be used to violate the classical relativity principle. We must then have

$$T_u(\lambda, v)_c = (\lambda', v')_c \tag{3.7}$$

where $v' \leq c$.

Stated another way, for the fractalons in O_c to obey the classical relativity principle, T_u must be an automorphism on O_c . We also notice that fractalons on the boundary of O_c (i.e. fractalons of the form $(\lambda, c)_c$) must remain on the boundary under an inertial transformation, i.e.

$$T_u(\lambda, c)_c = (\lambda', c)_c. \tag{3.8}$$

For T_u to preserve the boundary of O_c , T_u must depend on c . However, since T_u is a kinematic transformation and not dependent on the identity of a particle, c must be common to all particles. That is, if $(\lambda, v)_c$ corresponds to an observable particle (m_0, v) then all observable particles are such that $vw = c^2$, and O_c is the set of all observable particles. The phase diagram of such particles is sketched in figure 5.

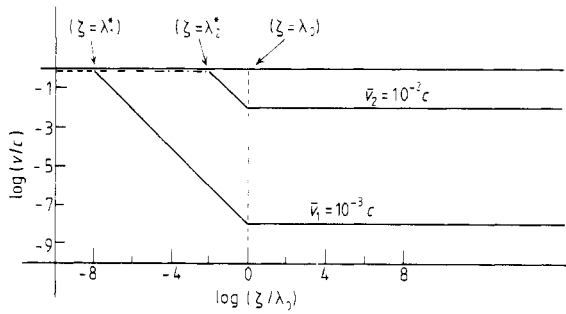


Figure 5. An idealised phase diagram for free fractalons. The ‘classical’ phase for $\zeta > \lambda_0$ is characterised by a scale-independent single-particle velocity. In the ‘Schrödinger regime’ for $\lambda^* < \zeta < \lambda_0$ the single-particle velocity is inversely proportional to scale. In the ‘field’ phase for $\zeta < \lambda^*$ particle velocities are scale independent but particle number is dependent on scale.

We notice that the diagram distinguishes two types of particles, ‘heavy’ particles such that $v < c$ and ‘light’ particles with $v = c$. The diagram also suggests that heavy fractalons have three phases. In the macroscopic phase, i.e. on scales above λ , v_x is independent of scale. On scales below λ but above τ we have a ‘Schrödinger’ phase where a single-particle description seems reasonable but where v_x is scale dependent. Finally on scales below τ a single-particle interpretation becomes inadequate, although particle velocities are scale independent.

In the following section we establish connections between the three phases.

4. Macroscopic correspondence

From figure 5 we see that free fractalons appear to move on classical one-dimensional trajectories when viewed on a scale greater than the fractal wavelength. That is, a

classical treatment of fractalons would appear justified provided both measurement and interaction occur on scales greater than λ . In § 3 we made the identification

$$(\lambda_0, v_0) \leftrightarrow (m_0, v_0) \tag{4.1}$$

where m_0 was taken as a macroscopic inertial mass that was invariant under an inertial transformation. This identification implied that there was an upper bound on macroscopic velocities c and a collection of ‘light fractalons’ that move with velocity c regardless of inertial frame. The existence of such light fractalons, along with the classical relativity principle, is sufficient to require T_u to be Lorentzian. This being the case, we identify m_0 with the rest mass of the particle.

Since T_u is Lorentzian, let us describe fractalons in the macroscopic regime by the relativistic mass

$$m_r = m_0 / (1 - v_0^2/c^2)^{1/2} \tag{4.2}$$

with macroscopic momentum

$$p = m_r v_0. \tag{4.3}$$

To determine the macroscopic significance of λ_0 for heavy fractalons let us make the assumption that m_r is independent of scale. With this assumption we may rewrite (2.2) as

$$\begin{aligned} m_r v(\eta) &= m_r v_0 (\eta/\lambda)^{1-D} \equiv p(\eta) & \eta \leq \lambda \\ \text{i.e.} \quad p(\eta) &= p_0 (\eta/\lambda)^{1-D} & \eta \leq \lambda. \end{aligned}$$

Retracing the derivation of (2.4), we may then write

$$\Delta x \Delta p_x \geq \frac{1}{3} \sqrt{5} p_0 \lambda_0. \tag{4.4}$$

We note that the LHS of (4.4) has no explicit dependence on the mass of the particle or its velocity. Thus the RHS must be a constant independent of mass and velocity, say $\sqrt{5}h/3$. This yields the relation

$$p_0 = h/\lambda_0. \tag{4.5}$$

Thus the fractal wavelength λ of a fractalon is inversely proportional to its macroscopic momentum, and the relativistic mass m_r is

$$m_r = p_0/v_0 = h/\lambda_0 v_0. \tag{4.6}$$

Substitution of (4.5) into (4.4) yields

$$\Delta x \Delta p_x \geq \sqrt{5}h/3. \tag{4.7}$$

Equation (4.6) apparently gives us a full prescription for making the identification (4.1) in the case of heavy fractalons. Light fractalons, on the other hand, have no ‘Schrödinger’-like regime for which we may write equation (4.4). However since λ is well defined for light fractalons let us assume that (4.5) also holds for light fractalons.

With (4.5) providing the link between ‘fractalons’ and macroscopic entities with momentum and velocity, we may incorporate relativistic mechanics into the macroscopic regime. We must, however, require that interactions and observations are restricted to scales greater than some λ_R , where λ_R is a representative wavelength of the system.

Let us develop relativistic mechanics in the macroscopic regime to arrive at the energy equation:

$$E = m_{\tau}c^2. \quad (4.8)$$

It is instructive to translate this relation into the 'fractal' representation. From (3.2) we have

$$c^2 = v_0 w_0 = v_0 \lambda_0 / \tau_0.$$

Thus, using (4.6), we have

$$E = m_{\tau} v_0 \lambda_0 / \tau_0 = h / \tau_0. \quad (4.9)$$

Defining $\omega_0 \equiv 2\pi / \tau_0$ and $\hbar = h / 2\pi$ this becomes

$$E = \hbar \omega_0 \quad (4.10)$$

where ω_0 is inversely proportional to the fractal wavelength in time for the fractalon. We also note that (4.8) implies the dispersion relation

$$E^2 = \frac{\hbar^2 c^4}{\lambda_0^2 v_0^2} = \frac{\hbar^2 c^2}{\lambda_0^2} + \frac{\hbar^2 c^4}{\lambda_0^2 v_0^2} \left(1 - \frac{v_0^2}{c^2}\right) = \frac{\hbar^2 c^2}{\lambda_0^2} + m_0^2 c^4$$

which also suggests that the rest mass on the light fractalon is zero, its energy being

$$E = hc / \lambda_0.$$

Finally, in order to interpret the fractal wavelength in time τ_0 directly, we note from (4.9) that

$$c\tau_0 = h / m_{\tau}c$$

is the 'Compton wavelength' of the fractalon.

5. Idealised fractal space-time versus geometry

In the above sketch of fractalon physics we have implicitly used idealised fractal space-time in which, for example, we have assumed that (2.1) and (2.2) hold without qualification as to the choice of length scales below λ . On the other hand, we have used the specific geometry of the Peano-Moore (PM) curve in order to interpret fractal time. We now investigate the compatibility of PM geometry with idealised fractal space-time.

If we require that a particle move on a planar PM curve, then the requirement that the particle have commensurate spatial and temporal trajectories is easily seen to be

$$v_0 = \left(\frac{1}{3}\right)^k c \quad k = 0, 1, 2, \dots$$

This is clearly unacceptable for heavy fractalons since we require continuously variable macroscopic velocities. Although one might tamper with the PM geometry, maintaining the dimension while changing the ratio of the wavelengths in the two perpendicular directions, we see that this would vary v_0 at the expense of altering the two wavelengths in a prescribed way. We suspect that such unwanted coupling of wavelengths would be a characteristic of any such regular and compact planar geometry since a fractal

curve with $D = 2$ is ‘plane filling’. However, since the analogous problem in quantum mechanics suggests that no particle with finite rest mass can be confined to a planar trajectory while maintaining a well defined relativistic mass, we consider embedding non-planar fractal trajectories in three-space.

For example, we may imagine a non-planar PM trajectory in which each self-similar figure is rotated through a random angle about its central axis. This curve would have the appropriate $D = 2$ while being non-planar. In three dimensions the spatial trail of a fractalon would have measure zero, and we might expect that, like a very loose ball of cotton, we might alter a wavelength in one direction, without changing the perpendicular wavelengths. In order to maintain synchronised space-time we could then require that on scales below $\lambda^* = c\tau$, the temporal trajectory be geometrically similar to the spatial geometry (with scale factor c). This would then require a topologically three-dimensional space in which to embed the temporal trajectory on scales below τ . Although such a six-dimensional space-time is not in common use as a description of physics, it has received some attention in relation to problems in special relativity (e.g. Cole 1980 and references therein).

We note that, in the above scheme, it is the extra two topological dimensions in time that allow us to consider the trajectory to be continuous, and since our objective is to try to preserve a single-particle continuous-trajectory description, we see that we have done so at the expense of our usual conception of a one-dimensional time. In any detailed attempt to construct a physical theory based on synchronised space-time trajectories, this aspect would require very careful examination.

However, if for the time being we accept that we may use a full six-dimensional space-time in which to invoke space-time synchronisation, the above non-planar PM curve appears to provide the correct qualitative features of idealised fractal space-time. We shall thus use the PM example as a guide for interpreting the behaviour of particles with more general microscopic geometries.

6. A random walk model

In previous sections we indicated a similarity between fractal space-time and quantum mechanics. The algebraic correspondence is illustrated in table 1.

In this section we attempt to construct field equation descriptions of fractalons. To do this we use a simple model in which the underlying geometry is that of a

Table 1.

Quantum mechanics	Fractal mechanics	Classical mechanics
λ (de Broglie)	λ (fractal wavelength)	—
λ_c (Compton)	$c\tau$ (fractal wavelength)	—
v_g (group velocity)	v (macroscopic velocity)	v
m (mass)	$h/\lambda v = m$	$m/[1 - (v^2/c^2)]^{1/2} = m_r$
v_{ph} (phase velocity)	$w = \lambda/\tau$	—
c (velocity of light)	c (velocity of light fractalons)	c
$p = h/\lambda$ (momentum)	$p = h/\lambda$	$p = m_r v$
$E = hv_{ph}/\lambda$ (energy)	$E = hw/\lambda = mc^2$	$E = m_r c^2$
$v_g v_{ph} = c^2$	$vw = c^2$	—
$\Delta x \Delta p_x > h/2$	$\Delta x \Delta p_x > \sqrt{5}(h/3)$	—

random walk with drift. This geometry has the advantage of being less artificial than the PM geometry, while having the correct fractal dimension.

In particular, we imagine a particle of mass m moving in the xy plane with macroscopic momentum $\mathbf{p} = (p_x, p_y)$. We model this motion by considering a particle moving on a two-dimensional lattice with lattice spacings Δx and Δy . For $\Delta x, \Delta y \gg \lambda_x, \lambda_y$ our lattice particle will hop in a regular sequence from lattice point to lattice point with a drift velocity of $\mathbf{v} = \mathbf{p}/m$. As we refine the lattice, eventually Δx (Δy) becomes of the order of λ_x (λ_y) and at this point we require that

$$\mathbf{v}(\Delta \mathbf{x}) \approx [v_x(\lambda_x/\Delta x), v_y(\lambda_y/\Delta y)] \quad \Delta x, \Delta y < \lambda_x, \lambda_y \tag{6.1}$$

with the additional requirement that the motion be a random walk with drift. We assume, by analogy with the PM trajectory, that (6.1) will result in an uncertainty relation for the particle, as well as defining the fractal wavelengths. In the usual description of a transition from a random walk to a diffusion equation, (6.1) is the requirement $\Delta t = O(\Delta x^2)$.

As we refine the lattice further we eventually have

$$\Delta x = \Delta y = h/mc = \lambda^* \tag{6.2}$$

at which point $v_x(\Delta x) = v_y(\Delta y) = c$.

In accordance with our use of fractal time, further refinement of the lattice requires the use of a synchronised temporal trajectory, so that the spatial trajectory of our particle becomes a cloud of particle-antiparticle pairs when viewed in one-dimensional time. We assume that this procedure will yield a particle with the correct macroscopic momentum and energy relationships as in previous sections. In order to create a field description of the process, we extract the following features from the PM example of figure 6(a).

In the figure we distinguish two types of vertices. Vertex a we call time-like since the particle experiences a synchronised space-time 'scattering' at that point. We note that inside area A, all the vertices are time-like, and if at some resolution $\Delta x \ll \lambda^*$ there is a density of ρ_x time-like vertices on the x axis, then the density of time-like vertices in area A is proportional to ρ_x^2 . Furthermore, the number of particles distinguishable at a given resolution is proportional to ρ_x^2 . We also note that all particles in area A move with speed c in the x direction.

Vertex b we call space-like because the trajectory changes direction in space at b while maintaining the same direction in time. We note that vertex b rotates the direction of motion by $\pi/2$ as the 'process' expands into area B. If ρ_y represents the density of time-like deflections along the y axis in area B then the number of particles in B is proportional to ρ_y^2 . Thus for this example we could consider a vector field $\boldsymbol{\rho}(X, Y, t)$ defined at intermediate points on the lattice, say $(x + \frac{1}{2}\lambda^*, y)$, $(x, y + \frac{1}{2}\lambda^*)$ where x and y are lattice points for the PM curve at resolution λ^* (e.g. e, b in figure 6). Here $\boldsymbol{\rho}$ would represent the linear densities of active time-like deflections along the relevant bond in (x, y) , the sign of $\boldsymbol{\rho}$ representing the direction of 'flow' of the process. In the PM example $\boldsymbol{\rho}$ could take on the five values $\boldsymbol{\rho} = \mathbf{0}, \pm\rho_x\hat{x}, \pm\rho_x\hat{y}$, and we would have

$$\sum_{XY} \boldsymbol{\rho}^2(X, Y, t) = \rho^2 \tag{6.3}$$

only one vertex being 'active' at any time t . We could then take $\boldsymbol{\rho}^2(X, Y, t)$ as a relative probability density.

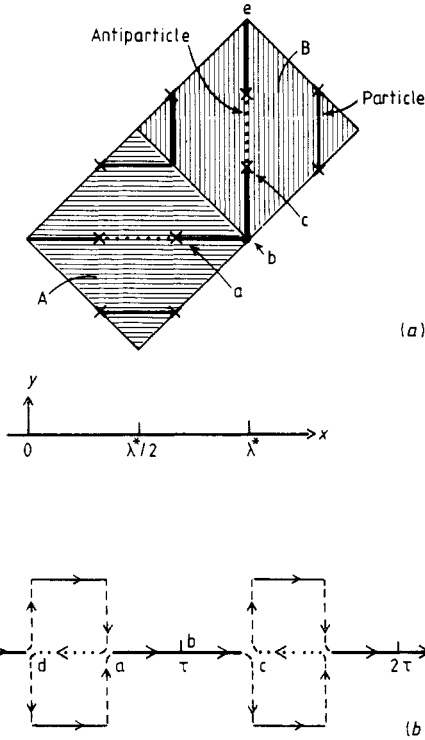


Figure 6. (a) The PM trajectory is initially confined to area A until the particle encounters vertex b. Thereupon the trajectory is rotated and confined to area B. Vertices like a and c are called time-like whereas vertex b is space-like. (b) The temporal trajectory of the particle in (a) with 'spin'. Note that the trajectory from τ to 2τ may be obtained from the trajectory from 0 to τ by a rotation of π about the t_{\parallel} axis.

We note that if we follow the motion of the fractalon, time-like collisions leave ρ unaffected whereas space-like collisions rotate ρ by $\pi/2$. In this example space-like collisions occur precisely every τ seconds, ensuring the maintenance of the PM geometry.

In the random walk model we maintain the description in terms of a vector density while removing the restriction that the space-like collisions occur precisely every τ seconds. Let us then consider the random walk case in which the lattice spacing is very much less than λ^* . On this scale all the particles will move with speed c and will only occasionally encounter space-like vertices. We assume that such collisions will affect rotations of ρ in proportion to their numbers. Thus, following the motion of the process, we will assume that ρ changes only through infinitesimal rotations so that we may write

$$\begin{aligned} \rho_x(X, Y, t + \Delta t) &= \rho_x(X - \Delta x, y, t) + A \Delta t \rho_y(x - \Delta x, y, t) \\ \rho_y(X, Y, t + \Delta t) &= \rho_y(X - \Delta x, y, t) - A \Delta t \rho_x(x - \Delta x, y, t). \end{aligned} \tag{6.4}$$

If we write ρ as a complex number this yields to first order

$$\partial \rho / \partial t = -c \partial \rho / \partial x - i A \rho \tag{6.5}$$

and similarly

$$\partial\rho/\partial t = -c \partial\rho/\partial y - iA'\rho. \tag{6.6}$$

Since (6.4) is an infinitesimal rotation A must be the angular frequency of space-like collisions. The expected value of A for the particle would then be

$$A = 2\pi \times \frac{(\text{total path length} - \text{expected displacement})}{\Delta x} \Big|_{\Delta x = \lambda^*}$$

$$= 2\pi[(c - v_x)/\lambda^*] = 2\pi(1/\tau - c/\lambda_x). \tag{6.7}$$

If we substitute the plane wave solution

$$\rho = \rho_0 \exp i(p_x x - Et)/h \tag{6.8}$$

into (6.5) we obtain the relation

$$E = p_x c + h/\tau - hc/\lambda_x. \tag{6.9}$$

Macroscopically we require that $p_x = h/\lambda_x$ so that (6.9) reduces to

$$E = h/\tau \tag{6.10}$$

which gives us the correct dispersion relation $E^2 = p^2 c^2 + m_0^2 c^4$. As in the PM case we assume that $\rho^*(x, t)\rho(x, \tau)$ is proportional to the expected particle-antiparticle density at a given scale, thus we might expect that $\rho^*\rho$ can be interpreted as a relative probability density for the particle.

However (6.8) is not the only solution to (6.5), the general solution taking the form

$$\rho(x, t) = \int d\Delta f(\Delta) \exp i[2\pi(x/\lambda_x - t/\tau) + \Delta(t - x/c)] \tag{6.11}$$

where $f(\Delta)$ is some suitable density.

This represents a superposition of plane waves of varying wavelength and frequency. The wave with $\Delta = 0$ has the correct macroscopic dispersion relation; however, the remaining waves have correct dispersion relations only if the 'rest mass' is made a function of Δ . To see why this is so we note that the quantity A in (6.4) has been chosen to be the 'constant' $2\pi(1/\tau - c/\lambda_x)$ in (6.7). However, macroscopically this constant is just

$$A = (2\pi/h)(E - pc) \tag{6.12}$$

which is not a relativistic invariant.

However, rewriting (6.5), we have

$$(\partial/\partial t + c \partial/\partial x + iA)\rho = 0. \tag{6.13}$$

Operating on the left with $(\partial/\partial t - c \partial/\partial x - iA)$ we have

$$\partial^2\rho/\partial t^2 - c^2 \partial^2\rho/\partial x^2 = (-A^2 + 2Aci \partial/\partial x)\rho. \tag{6.14}$$

Since the LHS of the equation is in covariant form we require that the operator on the RHS be covariant, with the additional requirement that A have the expected value assumed in (6.7) when operating on the plane wave solution (6.8). Substituting (6.8)

into (6.14) yields

$$\frac{\partial^2 \rho}{\partial t^2} - \frac{c^2 \partial^2 \rho}{\partial x^2} = \left(-4\pi^2 \left(\frac{1}{\tau} - \frac{c}{\lambda} \right)^2 - 4\pi \left(\frac{1}{\tau} - \frac{c}{\lambda} \right) p_x \right) \rho = \frac{1}{\hbar^2} (-E^2 + p_x^2 c^2) \rho = -\frac{1}{\hbar^2} m_0^2 c^4 \rho. \tag{6.15}$$

This equation has the desired relativistic invariance and the implied superposition is that of plane waves with identical rest masses. Equation (6.15) will be recognised as the Klein–Gordon equation for a spinless particle moving along the x axis. Similar arguments can be made for the projection onto the y axis of (6.6).

If we wish to extend the above model to three spatial dimensions, we change our underlying fractal trajectory to that of a random walk with drift in three dimensions. We may then write an equation of the form (6.4) where ρ_y is taken as the linear density of active time-like deflections along a line perpendicular to the x axis and in a plane defined by the direction of the infinitesimal rotation, which we assume to be slowly varying on this scale. This leads to three equations of the form (6.15) in the variables x , y and z which we may combine into the Klein–Gordon equation in three dimensions:

$$\hbar^2 (\partial^2 / \partial t^2 - c^2 \nabla^2) \rho = -m_0^2 c^2 \rho. \tag{6.16}$$

Although the passage from the concept of a synchronised space–time trajectory to the above equation is at best heuristic, we feel that the only major qualitative feature inherent in solutions of (6.16) that is not apparent in the original fractalon picture is the implied superposition principle. Although a superposition principle is hinted at by the uncertainty relation for fractalons, and the macroscopic requirement of relativistic invariance restricts the form of this principle, (6.16) is still an ansatz. We would like to point out that the consistency of this ansatz with the ‘geometric’ interpretation needs to be verified.

Equation (6.13) represents a synthesis of some of the qualitative features of the PM example, with an underlying stochastic geometry. However, one feature of the PM example that we did not model explicitly was the network of particles moving in a ‘perpendicular’ time direction. In figure 6(b) we note that the two particles and one antiparticle represented at time $\tau/2$ are a result of the components of the trajectory perpendicular to t_x at vertex d .

Let us model this behaviour in one dimension. In the previous model we represented the particle probability density by the square of the linear density of active time-like vertices which we called ρ_x . In order to include the part of the trajectories moving perpendicular to our time axis, we consider a complex density $\psi_1(x, t) = \psi_1^{\parallel}(x, t) + i\psi_1^{\perp}(x, t)$ in which $\psi_1^{\perp}(x, t)$ represents the linear density of time-like vertices along t_{\perp} . Similarly we will denote by $\psi_2(x, t) = \psi_2^{\parallel}(x, t) + i\psi_2^{\perp}(x, t)$ the densities perpendicular in space to the x axis, and we shall assume that the probability density is

$$P(x, t) \propto |\psi_1|^2 + |\psi_2|^2 = \psi_1^{\parallel 2} + \psi_2^{\parallel 2} + (\psi_1^{\perp 2} + \psi_2^{\perp 2}). \tag{6.17}$$

In the previous model we ignored the term in parentheses in (6.17) and assumed that ψ_1^{\parallel} and ψ_2^{\parallel} transformed in time as components of a vector under an infinitesimal rotation. That is, we assumed

$$\begin{aligned} \psi_1(x, t + \Delta t) &= \psi_1(x - \Delta x, t) + A \Delta t \psi_2(x - \Delta x, t) \\ \psi_2(x, t + \Delta t) &= \psi_2(x - \Delta x, t) - A \Delta t \psi_1(x - \Delta x, t) \end{aligned} \tag{6.18}$$

which would lead to the Klein–Gordon equation for both components ψ^{\parallel} and ψ^{\perp} .

However, one may modify the PM example as in figure 6(b) so that the rotation at point b becomes improper. To imitate this we modify (6.18) to incorporate an improper rotation i.e.

$$\begin{aligned} \psi_1(x, t + \Delta t) &= \psi_2(x - \Delta x, t) + ib \Delta t \psi_1(x - \Delta x, t) \\ \psi_2(x, t + \Delta t) &= \psi_1(x - \Delta x, t) - ib \Delta t \psi_2(x - \Delta x, t). \end{aligned} \tag{6.19}$$

We note that this transformation preserves the density (6.17) to $O(\Delta t)$. If we now write

$$\Psi = \begin{pmatrix} \psi_1 \\ \psi_2 \end{pmatrix}$$

and define the matrices

$$\alpha = -c \begin{pmatrix} 0 & 1 \\ 1 & 0 \end{pmatrix} \quad \beta = b \begin{pmatrix} 1 & 0 \\ 0 & -1 \end{pmatrix}$$

then, equating first-order terms in (6.19), we have

$$(I \partial/\partial t - \alpha \partial/\partial x - i\beta)\Psi = 0 \tag{6.20}$$

where I is the unit matrix. Operating on (6.20) from the left with $(I \partial/\partial t + \alpha \partial/\partial x + i\beta)$ we have

$$I(\partial^2/\partial t^2 - c^2 \partial^2/\partial x^2 + b^2)\Psi = 0.$$

This is consistent with the Klein-Gordon equation if we choose $b = m_0c^2/\hbar$. With this choice of b we see that (6.20) is a representation of the free-particle Dirac equation for one-dimensional motion.

It is interesting to note that the spinor character of the Dirac wavefunction arises, in the fractalon ‘picture’, from an improper rotation of the temporal trajectory at space-like vertices. In the PM version of figure 6(b), the temporal trajectory is rotated by π radians at vertex b about the t_{\parallel} axis. In (6.19) the temporal trajectory is rotated about t_{\parallel} with an angular frequency of $b = m_0c^2/\hbar$. In this picture particle ‘spin’ seems to correspond to the rotation of the temporal trajectory about the ‘observer’ time axis.

7. Conclusions

In §§ 1-5 we introduced the concept of fractal space-time through the use of synchronised PM trajectories. We noted that at least qualitatively plane filling spatial trajectories had several features in common with wavepackets. We then introduced synchronised fractal time which provided a mechanism whereby particle velocities could be made scale independent in spite of the fractal nature of spatial trajectories. We interpreted fractal time by assuming that only a one-dimensional projection of the temporal trajectory would be observable. On time scales below that of the fractal period of a particle, the two-dimensional nature of the temporal trajectory would be manifest in the appearance of particle-antiparticle pairs, the production of neutral pairs being guaranteed by the continuity of the trajectory. Throughout these sections we assumed that idealised fractal space-time was a reasonable and realisable abstraction of the PM example, and we used features of both to draw a correspondence between the wavelengths of fractalons and the wavelengths of quantum mechanical particles.

In order to maintain the continuity and synchronisation of the space–time trajectories of fractalons, we invoked the use of a three-dimensional time–space. The extent of the extra dimensions would be small for real values of c and h . For example, a non-relativistic electron would move in a time cylinder with a diameter of the order of 10^{-20} seconds. We note that the energy required to probe the extra dimensions of a particle's trajectory would be greater than the relativistic energy of that particle. However, we have not considered further implications of the extra dimensions in time, neither have we attempted a description in which the fractal trajectory of time is confined to one dimension.

In § 6 we extracted some qualitative features of fractal space–time and the PM example in order to construct two field equation descriptions. In the first equation we used the argument of requiring macroscopic relativistic invariance, in order to invoke an appropriate superposition principle. This resulted in the free-particle Klein–Gordon equation. For the second equation we constructed a one-dimensional model in which the 'density of time-like collisions' was allowed to advance through improper rotations. We found this to yield the one-dimensional free-particle Dirac equation.

Although our arguments have been mostly heuristic and the results consequently speculative, we feel that the objective of finding out to what extent the single particle–continuous trajectory paradigm can be maintained as a description of quantum phenomena is a legitimate objective. We hope this work will encourage interest in this question since we feel that the paradigm may not be as inadequate as hitherto supposed.

Acknowledgments

I would like to express my gratitude to Dr S G Whittington for his encouragement and financial support of this work. I should also like to thank Drs R Kapral and J A Gualtieri for helpful comments and criticisms of the manuscript.

References

- Abbot L F and Wise M B 1981 *Am. J. Phys.* **49** (1) 37
Camposino-Romeo E, D'Olivo J C and Socolovsky M 1982 *Phys. Lett.* **89A** (7) 321
Cole E A B 1980 *J. Phys. A: Math. Gen.* **13** 109–15
Feynman R P 1948 *Rev. Mod. Phys.* **20** (2) 367–87
Feynman R P and Hibbs A R 1965 *Quantum Mechanics and Path Integrals* (New York: McGraw-Hill)
Mandelbrot B B 1977 *Fractals: Form, Chance, and Dimension* (San Francisco: Freeman)